



WISP-2 expression induced by Teriparatide treatment affects *in vitro* osteoblast differentiation and improves *in vivo* osteogenesis



Alberto Smargiassi^{a,1}, Jessika Bertacchini^{b,*,1}, Marta Checchi^{b,**}, Francesco Potì^c, Elena Tenedini^d, Giuliana Montosi^e, Maria Sara Magarò^b, Emanuela Amore^b, Francesco Cavani^b, Marzia Ferretti^b, Grisendi Giulia^f, Delphine B. Maurel^g, Carla Palumbo^b

^a Indiana Center for Musculoskeletal Health (ICMH), University Building, Indianapolis, IN, USA

^b Department of Biomedical, Metabolic and Neural Sciences, Section of Human Morphology, University of Modena and Reggio Emilia, Modena, Italy

^c Department of Medicine and Surgery, Unit of Neurosciences, University of Parma, Parma, Italy

^d Center for Genome Research, Department of Medical and Surgical Sciences, University of Modena and Reggio Emilia, Modena, Italy

^e Center for Hemochromatosis, Department of Internal Medicine II, University of Modena and Reggio Emilia, Modena, Italy

^f Laboratory of Experimental Epileptology, Department of Biomedical, Metabolic and Neural Sciences, University of Modena and Reggio Emilia, Modena, Italy

^g Pharmaceutical Sciences Department, University of Bordeaux, BioTis, INSERM Unit 1026, Bordeaux, France

ARTICLE INFO

Keywords:

Bone cells
Wnt signaling
Teriparatide
Wisp-2

ABSTRACT

The Osteocyte, recognized as a major orchestrator of osteoblast and osteoclast activity, is the most important key player during bone remodeling processes. Imbalances occurring during bone remodeling, caused by hormone perturbations or by mechanical loading alterations, can induce bone pathologies such as osteoporosis. Recently, the active fraction of *parathormone*, PTH (1-34) or Teriparatide (TPTD), was chosen as election treatment for osteoporosis. The effect of such therapy is dependent on the temporal manner of administration. The molecular reasons why the type of administration regimen is so critical for the fate of bone remodeling are numerous and not yet well known. Our study attempts to analyze diverse signaling pathways directly activated in osteocytes upon TPTD treatment. By means of gene array analysis, we found many molecules upregulated or downregulated in osteocytes. Later, we paid attention to Wisp-2, a protein involved in the Wnt pathway, that is secreted by MLO-Y4 cells and increases upon TPTD treatment and that is able to positively influence the early phases of osteogenic differentiation. We also confirmed the pro osteogenic property of Wisp-2 during mesenchymal stem cell differentiation into the preliminary osteoblast phenotype. The same results were confirmed with an *in vivo* approach confirming a remarkable Wisp-2 expression in metaphyseal trabecular bone. These results highlighted the anabolic roles unrolled by osteocytes in controlling the action of neighboring cells, suggesting that the perturbation of certain signaling cascades, such as the Wnt pathway, is crucial for the positive regulation of bone formation.

1. Introduction

The bone tissue is a dynamic tissue that constantly undergoes modifications in response to physiological and pathological alterations (Hadjidakis and Androulakis, 2006; Raggatt and Partridge, 2010; Sims and Walsh, 2012), through bone remodeling (i.e. coupled bone resorption and bone formation). The bone cell population consists of two distinct lineages: the osteogenic lineage and the osteoclastic lineage. The maintenance of normal bone structure is driven by the intercellular cross-talk that occurs among bone cells. As proposed by many authors

(R. A. Dodds et al., 1993; Marotti and Palumbo, 2007; Skerry et al., 1989a,b) and largely demonstrated by Bonewald (2011) and Nakashima (Nakashima et al., 2011) osteocytes are considered the mechanosensors of bone (Bertacchini et al., 2017; Maycas et al., 2015; Nakashima et al., 2012) and are actively involved in orchestrating the function of both bone-forming osteoblasts and bone-resorbing osteoclasts. However, the role of osteocytes in osteoblast regulation, under both physiologic and pathologic conditions, is not fully characterized. Several lines of evidences indicate that osteocytes affect osteoblast differentiation and bone deposition in various ways: for example,

* Corresponding author.

** Corresponding author.

E-mail address: jb Bertacchini@unimore.it (J. Bertacchini).

¹ Equally contributing authors.

osteocytes regulate osteogenic response through IL-6 production via the STAT3 and ERK signaling pathway (Hao et al., 2017). Moreover, osteocytes subjected to Pulsating Fluid Flow stimulate the differentiation of osteoblasts *in vitro* via soluble factors such as TGF- β (Vezeridis et al., 2006). Of note, recently it has been shown that osteocytes can be considered as a source of anabolic factors such as Wnt1, able to speed up osteoblastogenesis by triggering Wnt signaling in osteoblasts (Joeng et al., 2017). It is also well known that osteocytes are a source of osteoprotegerin, the potent inhibitor of RANKL, that mediates the inhibition of bone resorption, but conversely they are also the producers of Sclerostin, the most important anti-anabolic regulator of bone formation by osteoblasts (Pietrzyk et al., 2017; Tatsumi et al., 2007; Weinstein et al., 2011; Xiong et al., 2014). During the last decade, in order to regulate the process of bone remodeling in osteoporotic patients, PTH (1-34), also known as TPTD, has been used as an anabolic drug (Bellido et al., 2013; Giannotti et al., 2013; Riek and Towler, 2011). The anabolic effects of parathormone involve a rapid increase in osteoblast differentiation and bone formation due to its ability to promote proliferation of osteoprogenitor cells, to inhibit osteoblast apoptosis and to activate lining cells in becoming active osteoblasts (Jilka, 2007; Kim et al., 2012). The effect of such therapy is dependent on the type of administration, in fact it has been largely demonstrated that a short administration of TPTD increases bone mass but a long administration leads to an increased bone resorption. The molecular reasons why the type of administration regimen is so critical for the fate of bone remodeling are not well known. It has been proven that the short administration of PTH (1-34) induces osteoblast hyperplasia, increases osteoblast survival and augments their ability to differentiate and to induce matrix mineralization. On the contrary, long term treatment with PTH (1-34), leads to the increment of osteoclast numbers and to the increase of their activity during bone resorption (Guimarães et al., 2013; Neer et al., 2001; Osagie-Clouard et al., 2017; Poole and Reeve, 2005; Sugiura et al., 2015). The molecular mechanisms occurring in osteocytes during treatment with PTH (1-34) are poorly known; reports published so far contradict each other, thus the activity of this hormone on osteocytes has not yet been elucidated as well as its ability to modulate some signaling pathways (Iida-Klein et al., 2005). In fact, the role of the Wnt signaling pathway (the most important pathway activated in bone tissue) in the mechanical adaptation of bone, has been studied predominantly in osteoblasts but not in osteocytes, and it is still unclear whether osteocytes can produce Wnt in response to different stimuli. The Wnt canonical signaling pathway affects cellular processes by regulating β -catenin levels and its subcellular localization (Angers and Moon, 2009; Mao et al., 2001). Upon binding of extracellular Wnt to LRP5/6 and frizzled co-receptor complex, Dishevelled (Dsh) is activated, causing Axin recruitment to the membrane and inactivation of glycogen synthase kinase-3 β (GSK-3 β) that induces, in turn, the stabilization and accumulation of β -catenin in the cytoplasm (Bertacchini et al., 2018). Stabilized β -catenin translocates to the nucleus and activates transcription. Physiological responses result in the increased expression of Wnt pathway and Wnt/ β -catenin target genes including Wnt10B, SFRP1, cyclin D1, Fzd2, Wisp-2, and connexin. Among these, it is particularly interesting and not well investigated Wisp-2, that is a member of the Wnt1 inducible signaling pathway protein subfamily, which belongs to the connective tissue growth factor (CTGF) family. It may play an important role in modulating bone turnover; in particular, it: 1) promotes the adhesion of osteoblast cells, 2) inhibits the binding of fibrinogen to integrin receptors and 3) inhibits osteocalcin production. This notwithstanding, Wisp-2 role in osteocyte-mediated signaling is unknown (MacDonald et al., 2009) (Robinson et al., 2006). Therefore, the current study is aimed to clarify the role of the osteocyte in the changes induced by TPTD administration and will attempt to identify the molecular differences that occur between the various effects (i.e. fast or retard) of drug administration. For the first time, our data indicate the osteocytes as producers of Wisp-2, as a molecule with a great osteogenic power able to modulate the activity of the neighboring cells,

such as osteoblast or bone lining cells. Through this mechanism, we focus our attention on one of the possible ways by which the osteocytes may regulate the differentiation of mineralized tissues when exposed to TPTD, thereby emphasizing one of the possible important functional roles that this cell type has in bone remodeling and, more generally, in skeletal metabolism.

2. Materials and methods

2.1. Cell lines culture

Murine Long bone Osteocyte Y4 (MLO-Y4) were provided by Prof. Lynda Bonewald (IU School of Medicine - Indiana University, Indianapolis) and were cultured on collagen pre-coated (GIBCO) tissue culture plates and grown at 37 °C, 5% CO₂, (95% air), using DMEM (Euroclone) containing ribonucleosides, deoxyribonucleosides, and L-glutamine, supplemented with 5% FBS (Euroclone), 5% CS (Euroclone) and penicillin/streptomycin at 100 U/ml. Cells were initially thawed and plated in 6-well plates at a concentration of 150.000 cells/well and then subcultured once they reached 80% of confluence. MLO-Y4 cells were cultured for different times (6, 9 or 12 h) with and without 10 nM of TPTD (Eli Lilly, USA). At the end of treatment, cells were collected, washed in PBS and stored at -20 °C. In parallel, the conditioned medium from samples were collected and stored at -80 °C.

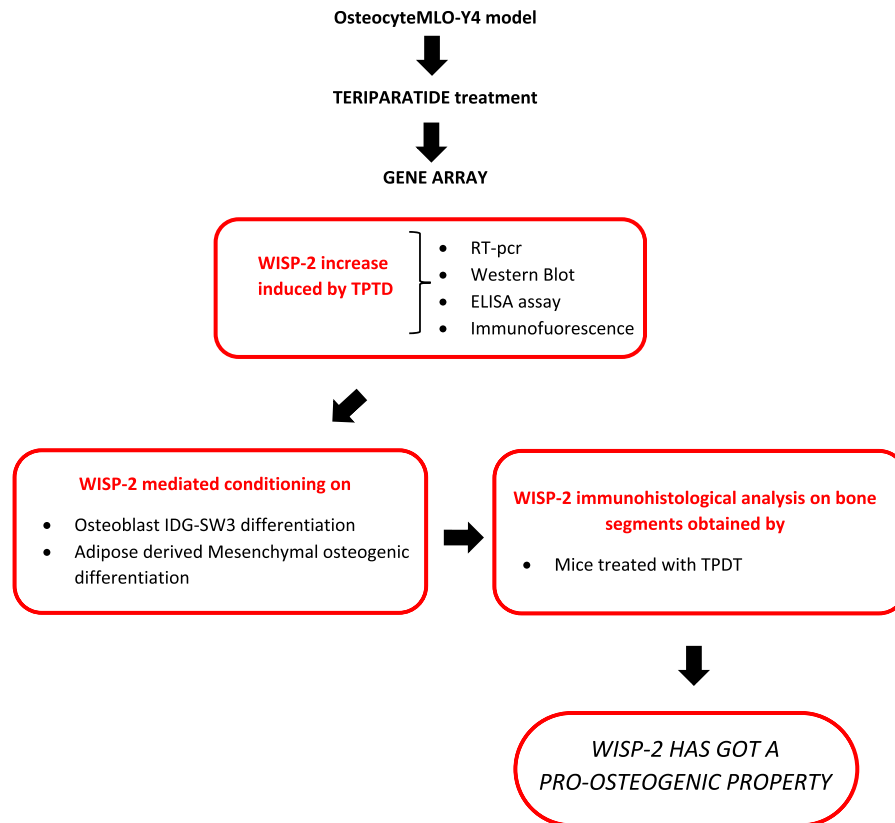
The murine IDG-SW3 osteoblast cell line was also obtained by Prof. Lynda Bonewald. Cells were plated at 1×10^4 cells/cm² and cultured as previously described (Woo et al., 2011). These cells are immortalized with a temperature sensitive T-antigen that is induced by interferon gamma (IFN- γ), therefore they proliferate under permissive conditions (33 °C in α -MEM with 10% FBS, 100 U/ml penicillin, 50 μ g/ml streptomycin) and 50 U/ml IFN- γ on type I collagen-coated plates. IDG-SW3 cells were cultured under proliferative conditions and when the cultures reached confluence, the medium was replaced with osteogenic differentiation medium (α -MEM with 10% FBS, 100 U/ml penicillin, 50 μ g/ml streptomycin, 50 μ g/ml ascorbic acid and 4 mM β -glycerophosphate) without IFN- γ and with the addition of MLO-Y4 conditioned medium in a ratio of 1:5. Cells were cultured at 37 °C and the medium was changed every three days. Viability of MLO-Y4 cells treated with TPTD at different concentrations was determined by the 3-(4,5-dimethylthiazol-2-yl)-2,5-diphenyltetrazolium bromide (MTT)-based colorimetric assay. The absorbance was read at OD = 570 nm. Mesenchymal Stem cells were kindly provided by Prof. Massimo Dominici (UNIMORE, Modena, IT) and were cultured in α -MEM plus 100 U/ml penicillin, 50 μ g/ml streptomycin, 2.5% of Human Platelet Lysate and 0.2% of Heparin. Osteogenic differentiation medium was the same used for IDG-SW3 cells.

2.2. Real-time RT-PCR

Reverse transcription was performed with First-strand cDNA Synthesis kit (Origene) using aliquots of total RNA extracted for microarray analysis. The cDNA samples were diluted to 20 ng/ μ l and the amplifications were done using the Sens Mix SYBR Master Mix (Origene).

Osteoprotegerin primers were: For 5'-TGGCACACAGTGATGAAT GCG-3'; Rev 3'-GCTGGAAAGTTTGCTCTTGCG-5'; **RUNX2** primers were: For 5'- TTAATCCACAAGGACAGA-3' Rev 3'-GTAAGACTGGTCA TAGGA-5'. **SOST** primers were For 5'- TGAGACAACCAGCCAT-3', Rev 3'- ACATCTTTGGCGTCATAG-5'; **WISP-2** primers were: For 5'-TGTGACCAGGCAGTGATG-3', Rev 5'-AGTGACAAGGGCAGAAAGT-3' **GADPH** primers were For 5'-GGCATTGCTCTCAATGACAA-3'; Rev: 5'-ATGTAGGCCATGAGGTCCAC-3'. The primers were used at the concentration of 0,5 μ M. The thermal cycling conditions were 50 °C for 2 min followed by an initial denaturation step at 95 °C for 10', 45 cycles at 95 °C for 30", 60 °C for 30" and 72 °C for 30". The experiments were carried out in triplicate for each data point. The relative quantification

Table 1
Experimental workflow.



in gene expression was determined using the $2\Delta\Delta C_t$ method (Livak and Schmittgen, 2001). By means of this method, we obtained the fold changes in gene expression normalized to an internal control gene GAPDH, and relative to each line (calibrator).

2.3. Gene expression

The total cellular RNA was isolated from the samples previously collected using RNeasy RNA isolation kit (Qiagen, Hilden, Germany) following the manufacturer's recommendations. Disposable RNA chips (Agilent RNA 6000 Nano LabChip kit, Agilent Technology, Waldbronn, Germany) were used to determine the concentration and purity/integrity of RNA samples using Agilent 2100 bioanalyzer. cDNA synthesis, biotin-labeled target synthesis, GeneChip® Mouse Genome 430 2.0 arrays hybridization, were performed according to the standard protocol supplied by Affymetrix (Affymetrix, California, USA). The amount of transcript mRNA (signal) was determined by the MAS 5.0 absolute analysis algorithm. All expression values for the genes in the MAS 5.0 absolute analyses were determined by using the global scaling option. Alternatively, probe level data were converted to expression values using robust multi-array average (RMA) procedure. Perfect match values were background adjusted, normalized using invariant set normalization and log transformed. The RMA-generated data were uploaded onto GeneSpring software version 7.2 using the log 2 transformation procedure. Supervised analyses were performed using the analysis of variance (one-way ANOVA) test (Welch ANOVA at a confidence level of 0.05) with the Benjamini and Hochberg correction of the false discovery rate, and using dChip Compare Sample procedure.

2.4. Western blot procedure and ELISA assay

Cells were collected and diluted in Lysis buffer (50 mM Tris-Cl, pH 7.4, 150 mM NaCl, 1% NP40, 2 mM EDTA, Protease Inhibitor Cocktail). Proteins extracted were quantified with Bradford assay. SDS-PAGE was performed according to Laemmli's procedure. Next, gels were blotted onto nitrocellulose membranes subsequently incubated overnight at 4 °C with the following primary antibodies (all from Santa Cruz Biotechnology, USA): anti-Pleiotropin (rabbit polyclonal, 1:250); anti-Connective Tissue Growth Factor/CTGF (rabbit polyclonal, 1:250); anti-Wisp-2 (rabbit monoclonal, 1:250); anti-Serpine1/PAI-1 (rabbit polyclonal, 1:250), anti-cathepsinK/CTSK (rabbit polyclonal, 1:250), anti-Actin (rabbit polyclonal, 1:250), anti-active β -catenin (Merck 1:2000).

Then, the membranes were incubated with a solution containing 1:2000 dilution of horseradish peroxidase (HRP)-conjugated secondary antibody (DakoCytomation, Denmark). Target bands were visualized using a mix of peroxidase solution plus a luminol enhancer solution (WesternSure™ PREMIUM Chemiluminescent substrate). Result acquisition and band densitometric analysis (represented by arbitrary units, AU), were performed using the C-DiGit® Blot Scanner (LI-COR Biosciences, NE, USA) and the Image Studio Lite 5.0 software (LI-COR Biosciences, NE, USA). All values were compared to respective normalized control levels. Analysis of proteins secreted in conditioned medium was obtained by centrifugation at 3000 rpm for 1 h at 4 °C in Amicon® Centrifugal Filter Devices and run in SDS-PAGE in equal amount of volume.

Wisp-2 Elisa assay was performed based on the manufacturer's instructions provided by mouse Wisp-2 Elisa kit (Fine Test).

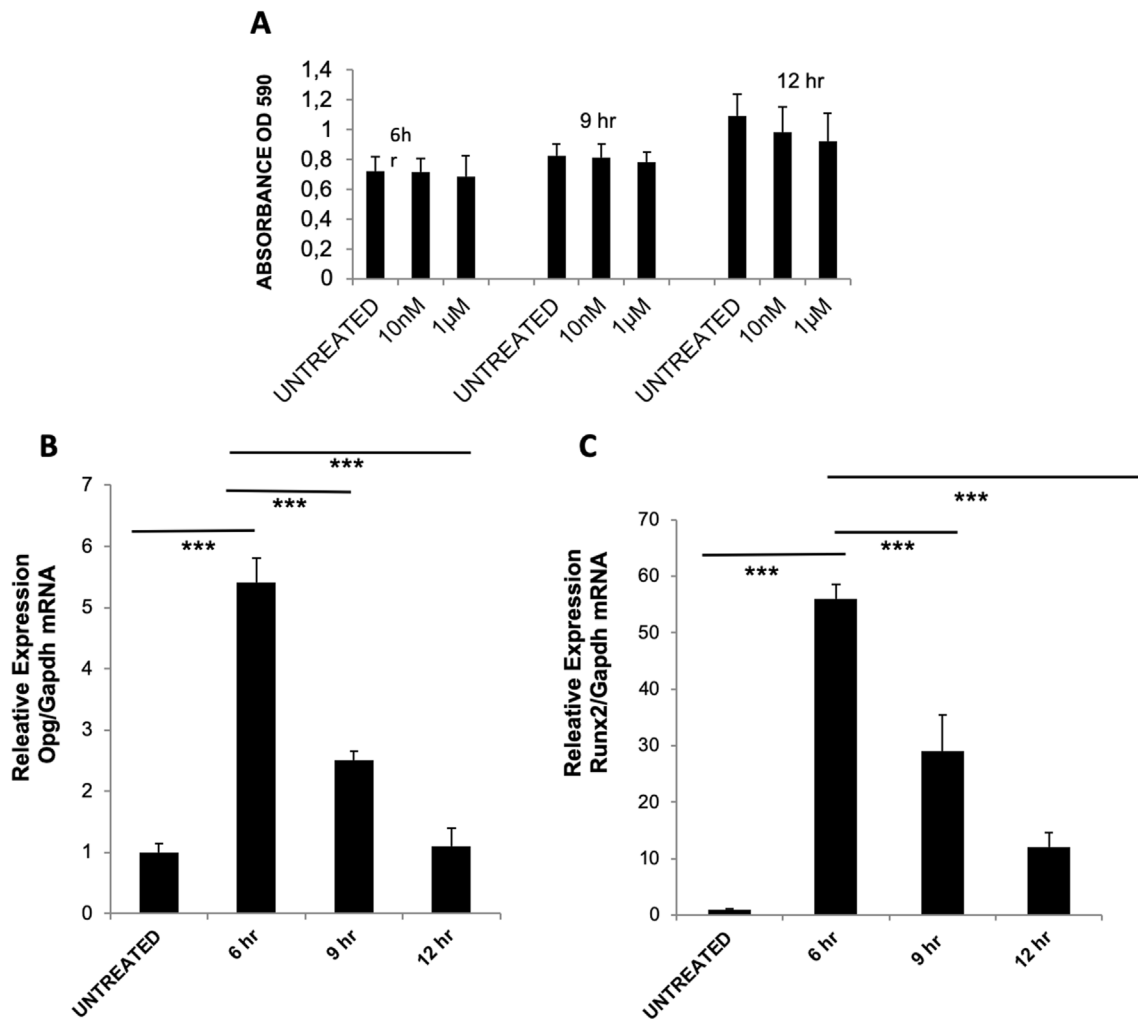


Fig. 1. A: MTT assay to measure cell viability (at 570 nm) of MLO-Y4 cells cultured for 24 h and treated for 6, 9 and 12 h with Teriparatide 10 nM and 1 µM. B-C: Total mRNA was extracted from MLO-Y4 cells treated with Teriparatide 10 nM for the indicated times and RUNX2 and Osteoprotegerin mRNAs were amplified by specific primers. Fold change variation was calculated. The data are representative of three independent experiments. The error bars show ST-DEV. Student T-test was performed. *** $p < 0,005$.

2.5. Immunofluorescence

MLO-Y4 cells, grown on glass coverslips, were fixed in 4% paraformaldehyde at 4 °C for 20', blocked in 4% BSA-PBS and incubated with primary antibody Wisp-2 overnight at 4 °C. Coverslips were next washed with PBS and incubated with fluorescence-labeled secondary antibodies (Thermo Scientific) for 1 h at room temperature. Slides were washed and mounted with DABCO 10% solution and observed with a Nikon E600 fluorescence microscope equipped with a digital camera. All the images shown in this paper are representative of at least 3 independent experiments carried out under the same conditions. Images from immunofluorescence studies were processed using Adobe Photoshop CS 8.0 software (Adobe Systems, San Jose, CA, USA).

2.6. Alizarin red and ALP assay

The IDG-SW3 cells were cultured in 6-well plates at 10^5 cells/cm² and cultured in proliferative media until they reached confluence, after that the medium was switched to differentiation medium and changed every three days. Media collected from MLO-Y4 cells obtained after treatment with TPTD for 6, 9 and 12 h, were diluted in the differentiation medium for IDG-SW3 cells. After 7, 14 and 21 days of osteogenic differentiation, the media were removed and the cell monolayers were gently washed 3 times with PBS. The cells were fixed in

10% buffered formalin for 10 min at 4 °C. After this time, fixative solution was removed, cultures were washed in PBS and plates were stored in PBS at 4 °C until sample processing. PBS was removed from the stored plates and the cell layer was stained with 2% Alizarin-S (Sigma-Aldrich, St Louis, MO, USA) at ~ pH 4.2 for 5'. Cell preparations were washed with PBS to eliminate non-specific staining. To quantify calcium deposition, the dye was removed from the monolayer by the addition of 10% cetylpyridinium chloride solution until all the dye had been drawn from the monolayer. A volume of 200 µl of the solution (in duplicate) was transferred to a clean 96-well plate. Optical density was measured by spectrophotometry at 570 nm, using 10% cetylpyridinium chloride as a blank reference. All values were compared to respective normalized control levels. The differentiation of IDG-SW3 cells was evaluated as a function of ALP activity after 5 days. ALP activity was assessed using an Alkaline Phosphatase Assay Kit (Colorimetric, Abcam, USA, ab83369) according to the manufacturer's instructions. Briefly, cells were grown on 6-well plates at a density of $1,5 \times 10^5$ cells per well. The medium was replaced after 24 h by α -MEM containing 10% FBS, 50 µg/ml ascorbic acid and 4 mM β -glycerophosphate (osteogenic medium) to induce osteoblast differentiation. Cells were collected from each treatment group and homogenized with assay buffer. The homogenized cellular lysate was then centrifuged at 13,000 g for 15 min to remove insoluble cellular debris. Afterward, ALP activity was determined with respect to the release of p-nitrophenol from p-

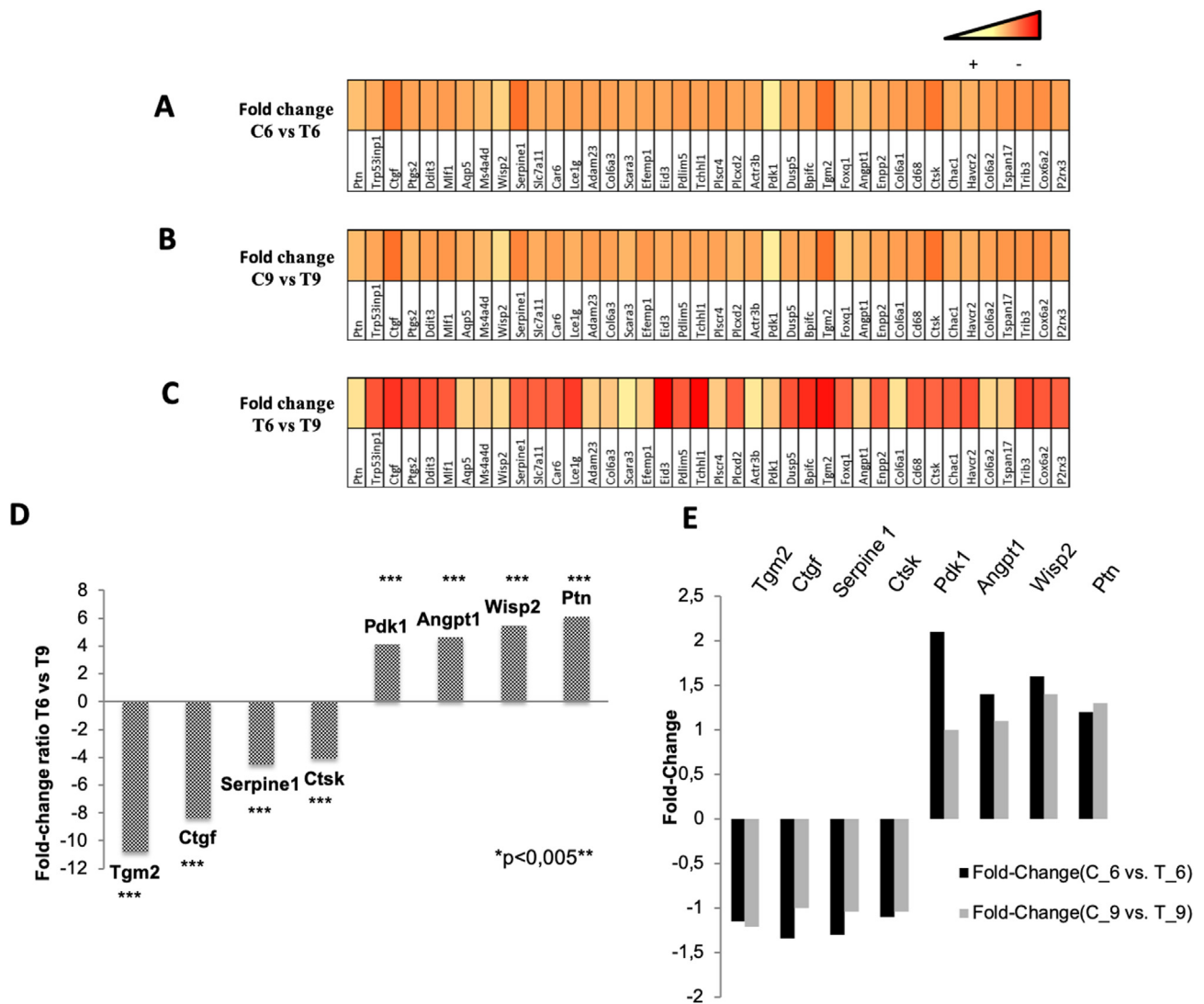


Fig. 2. A-B-C: Gene array was performed on MLO-Y4 cells treated with Teriparatide 10 nM for 6 and 9 h. The comparison between control and treated samples (C6 vs T6 - C9 vs T9 - T6 vs T9) were shown in the heat maps. D: Bar chart showing the most important genes involved in bone processes. Y-AXIS shows the fold change variation between T6 and T9 samples. E: Bar chart showing the most important genes involved in bone processes. Y-AXIS shows the fold change variation between C6 vs T6 and C9 vs T9 samples.

nitrophenyl phosphate substrate: an aliquot of supernatant was collected from each sample and added into the pre-labeled 96-well plate with subsequent addition of 50 µl of 5 mM pNPP solution into each well. The 96-well plates were then incubated at 25 °C in the dark for 60 min followed by the addition of 20 µl of stop solution into each well. Optical density was measured at 390 nm using a Thermo Scientific Appliskan™ plate reader (Thermo Fisher Scientific, 168 Third Avenue, Waltham, MA, USA).

2.7. Experimental animals

Three-month-old Sprague Dawley male rats (n = 9) were purchased from Charles River Laboratories (Calco, Lecco, Italy). At the time of arrival, all rats were housed individually in single cages, to better check food intake of each rat, and maintained under laboratory controlled conditions (22 ± 1 °C, 55–60% humidity, 12 h light:12 h dark). After seven days of acclimation to housing conditions, the rats were randomized into three groups of 3 animals each (Fig. 1), indicated as follows. Group 1 (control): fed normal diet and natural water ad libitum for 8 weeks. Group 2: fed calcium-deprived diet and distilled water ad libitum for 4 weeks and successive normal diet restoration and natural

water ad libitum for 4 weeks; group 3: fed calcium-deprived diet and distilled water ad libitum for 4 weeks and successive normal diet restoration and natural water ad libitum for 4 weeks with concomitant administration of PTH (1-34) 40 µg/kg/day. The calcium-deprived diet is a casein-based synthetic diet containing a very low amount of calcium (0.04% Ca). PTH (1-34) was supplied by Eli Lilly and Company (Indianapolis, USA), solubilized in saline (40 µg/mL) and subcutaneously injected in a volume of 100 µL/100gr body weight per rat.

2.8. Immunohistochemical and histomorphometrical analysis

Immediately after euthanasia, the right femur of each animal was removed, deprived of soft tissues, fixed in sodium phosphate-buffered (PBS) 4% paraformaldehyde pH 7.4, and decalcified in 10% EDTA solution for 30 days. Bones were then washed with PBS, dehydrated in graded ethanol, and embedded in paraffin. Femur distal metaphyseal trabecular bones were longitudinally cut with a Leica SP 1600 diamond saw microtome cutting system (Leica SpA, Milan, Italy) to obtain 4 µm thick sections. For immunohistochemical analyses the 3 tissue sections from each sample were permeabilized with 0.3% Triton X-100, blocked for intrinsic peroxidase activity with 3% hydrogen peroxide for 10 min,

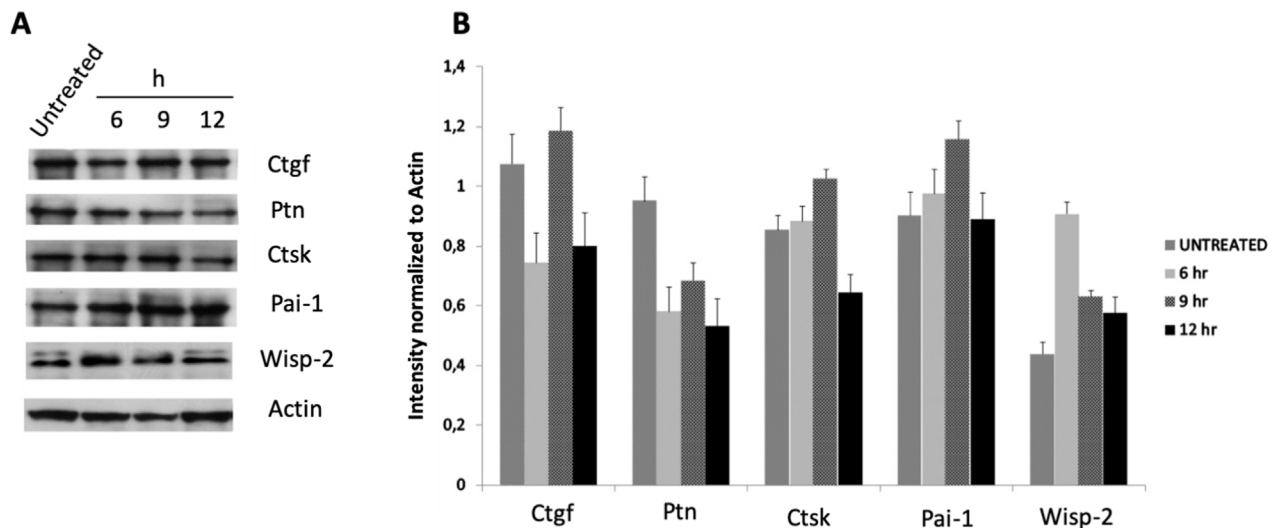


Fig. 3. A: SDS-PAGE and immunoblotting analyses of 10 μ g of MLO-Y4 protein extracts (as indicated). B: Optical density measurements. Statistical analysis made by Student T-test.

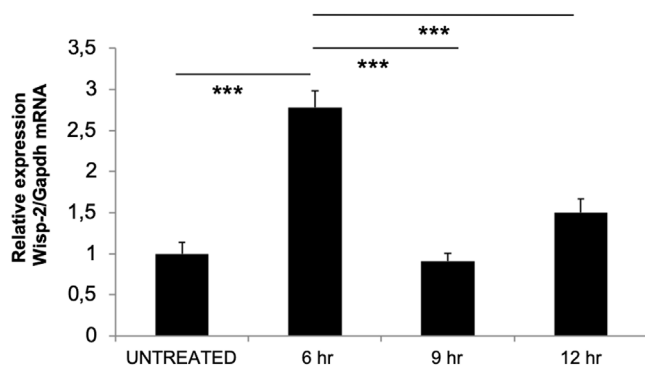


Fig. 4. Relative expression of Wisp2 mRNA: total mRNA was extracted from MLO-Y4 cells treated with Teriparatide 10 nM for the indicated times and WISP-2 mRNA was amplified by specific primers. The data are representative of three independent experiments. The error bars show ST-DEV. Student T-test was performed. *** $p < 0,005$.

and processed for heat-mediated antigen retrieval with Tris-EDTA (10 mM Tris Base, 1 mM EDTA Solution, 0.05% Tween 20, pH 9.0). Then, the slides were blocked in 10% normal serum with 1% BSA for two h at room temperature and incubated with primary antibody (AM31932PU-N WISP2 ACRIS) at 4 °C for 16 h. For detection of Wisp-2, the sections were incubated with secondary antibody anti-rabbit-HRP (Thermo Scientific) and the binding of peroxidase-conjugated secondary antibodies was detected with a DAB kit (Vector Lab, Peterborough, United Kingdom). For histomorphometrical analysis, after paraffin embedding, three sections (4 μ m) were obtained from each sample and stained with Hematoxylin & Eosin (H&E). Slides were deparaffinized by means of two changes of xylene for 5 min each, hydrated through a graded series of alcohol (100%, 95%, 80% and 70%) for 5 min each and rinsed first in tap water and then, in deionized water 1 min each. After dehydration procedure, the slides were stained in Carazzi hematoxylin solution (DiaPath C0203), rinsed in tap water, stained in alcoholic 0,5% eosin Y (DiaPath C0353) and rinsed in deionized water 1 min each. After dehydration through a graded series of alcohol (70%, 80%, 95% and 100%) for 5 min each and an incubation in xylene for 10 min, each slide has been mounted using DPX mounting solution (06522 Sigma Aldrich).

Stained sections were evaluated with Axiophot (ZEISS) microscope equipped with a DS-Fi3 camera (Nikon) and processed with NIS-Elements D 5.11.00 software (Nikon). WISP-2-positive cells on the

trabecular bone area were counted (N/area expressed in percentage value) as demonstrative of WISP-2 expression. The extent of the surface of prismatic osteoblast laminae was measured with respect to the metaphyseal trabecular surfaces (Ob.S/BS expressed in percentage value) as indicative of osteogenesis occurrence.

2.9. Statistical analysis

Data are expressed as means of duplicate biological experiments. Within each group (control, 6, 9 and 12 h treatments), differences were tested using a one-way analysis of variance (ANOVA), with a p -value of 0.05 to consider the differences as statistically significant. Student–Newman Keuls post-tests were employed to assess differences between groups. All values are reported as the mean \pm standard deviation (SD). T-student test was applied with $p < 0.05$. Data were analyzed by using Prism 5 (Graphpad Software Inc., La Jolla, CA).

3. Results

3.1. Gene expression profiling of MLO-Y4 cell line upon Teriparatide treatment

The osteocyte-like cell line (MLO-Y4) was selected for the study since it shows a good expression of most of the typical osteocyte differentiation markers. To explore a specific gene signature for TPTD treated cells, we conducted a gene array experiment. In order to select the concentration of TPTD that did not affect cell viability, MLO-Y4 were cultured for 24 h and treated for 6, 9 and 12 h with two different drug concentrations, 10 nM and 1 μ M, respectively. At the end of the treatments, cell viability was monitored by MTT assay: the results showed good tolerance of MLO-Y4 cells to the drug at any concentration used; no differences in terms of proliferation were shown (Fig. 1A), therefore in order to restrict eventual side effects the lowest concentration was selected to perform further experiments.

In order to confirm whether TPTD was been efficacious, a time course experiment was performed. MLO-Y4 cells were treated with TPTD at 10 nM for 6, 9 and 12 h and the mRNA of the well-known osteoclastogenesis inhibitory factor, Osteoprotegerin (OPG), was monitored by quantitative PCR. As expected, the OPG level was increased upon 6 h, then it dropped to the levels of untreated cells upon 9 and 12 h (Fig. 1B).

In parallel, the mRNA levels of RUNX2, a key transcription factor associated with osteogenic differentiation, were analyzed. The results

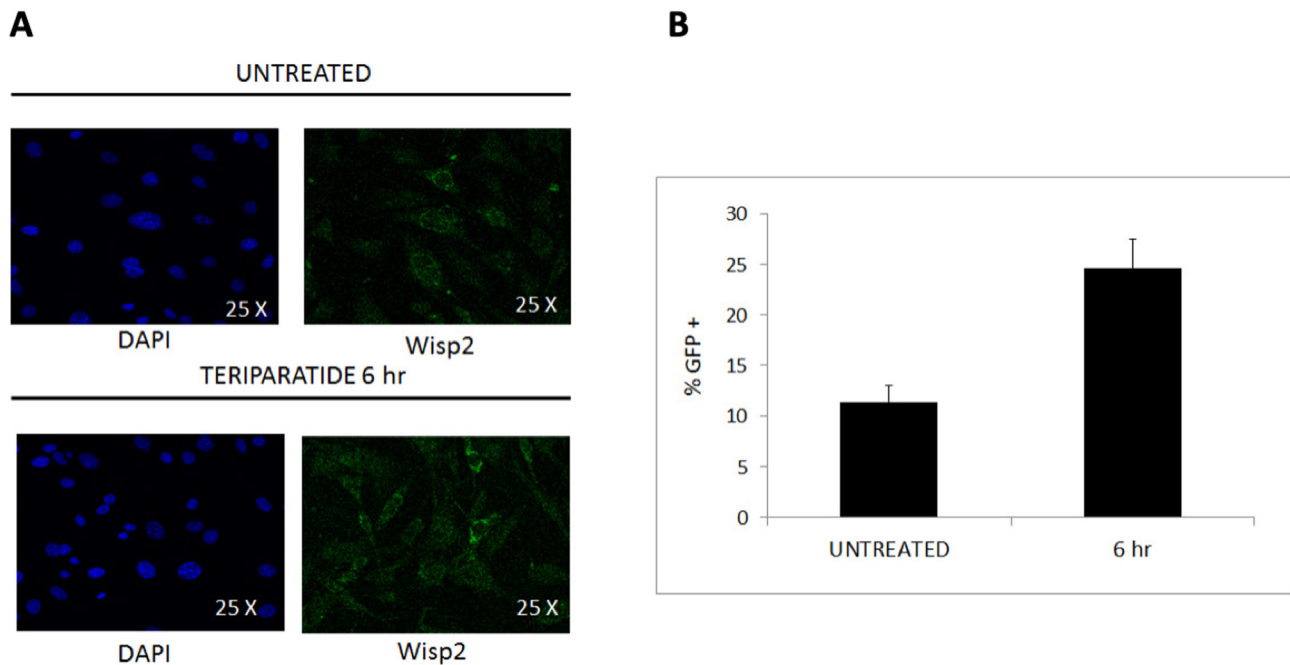


Fig. 5. A: Immunofluorescence images showing the localization of WISP-2 in cultured MLO-Y4 cells treated with Teriparatide 10 nM for 6 h. Magnification is 25 x. **B:** The number of GFP positive cells (expressed as percentage value) was calculated on 5 different fields and it was normalized to the number of total cells stained with DAPI. We counted as positive, all cells that exhibited detectable fluorescence; cells that did not express GFP had no fluorescence.

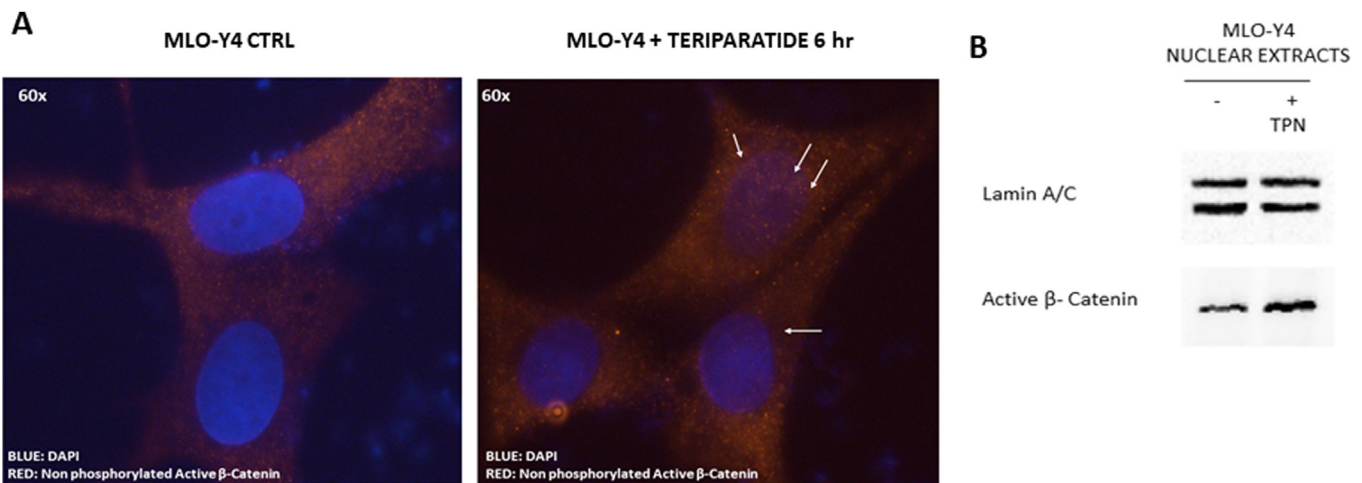


Fig. 6. Immunofluorescence images showing: A the localization of active β -Catenin in cultured MLO-Y4 cells treated/untreated with Teriparatide 10 nM for 6 h; **B** probed proteins (as indicated) from 20 μ g of nuclear extracts resolved in SDS-PAGE. Magnification is 60X.

turned out to be in line with the detected OPG levels, indicating a great induction of RUNX2 upon TPTD 6h treatment, with a decreasing transcription upon 9 and 12 h (Fig. 1C). Next, in order to investigate the molecular mechanisms activated by TPTD in MLO-Y4 cells, a basal gene expression analysis was performed after 6 and 9 h of treatment. A huge amount of data was obtained and analyzed statistically with Anova test (data not shown). The transcriptomes of drug treated samples (either for 6h and 9h) showed variations, suggesting that the drug affects the whole genome layout.

The comparison between treated samples (T6 vs T9) showed a consistent differential gene expression of more than 4-fold (log ratio 2.0) for 40 genes shown in Fig. 2C. The fold change, mentioned above, was kept intentionally high to restrict the field and avoid possible bias. Differences between control and treated samples were shown with low variations not statistically significant (Fig. 2A-B). The genes predominantly involved in bone processes, such as bone erosion and bone

formation, are summarized in Fig. 2D. From the preliminary gene array experiments, it emerged a high up-regulation of several genes involved in bone anabolism processes; in parallel, genes involved in the bone remodeling process were downregulated upon TPTD treatment. The bar charts demonstrated an inversion of gene expression between the two times selected, suggesting a possible role of these genes in a regulatory mechanism. Next, we compared the expression of these genes in treated samples (T6-T9) versus control samples (C6-C9) and we did not find any significant differences although there are interesting trends (2E). (See Table 1)

3.2. Wisp-2 expression analysis in MLO-Y4 osteocytes

In order to validate the results of the gene array and to verify precisely the different expression of some genes, protein levels of CTGF, PTN, CTSK, PAI-1 and WISP-2 were evaluated by western blot.

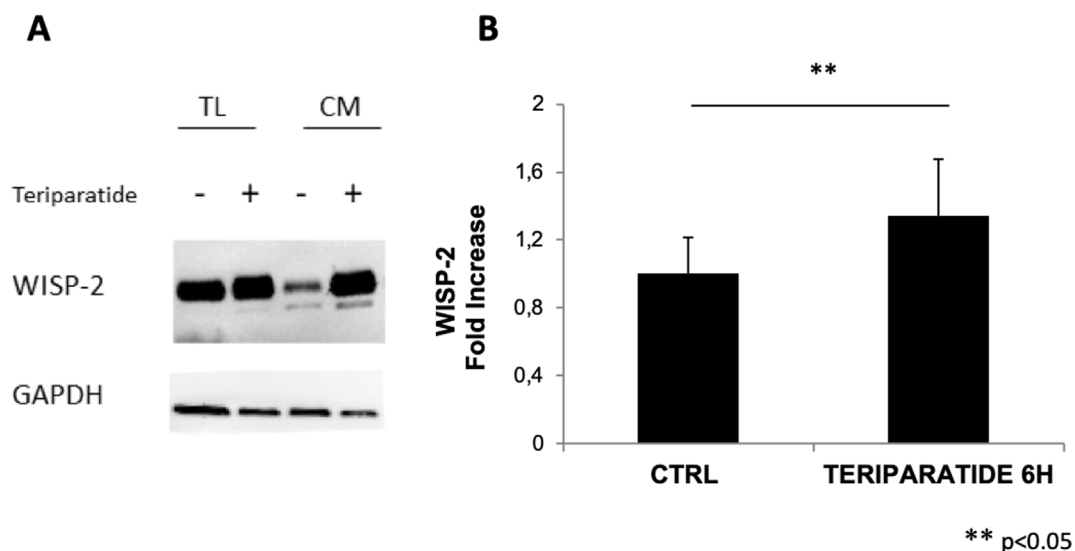


Fig. 7. A: Western blot analysis of MLO-Y4 cells treated or not with Teriparatide. TL total lysates (20 μ g), CM conditioned medium. **B:** Quantification of WISP-2 protein in conditioned medium by ELISA assay.

Intentionally, a further continuous time of 12 h of treatment was selected in order to ensure complete translation between mRNA and protein (Fig. 3A and B). We found that, all proteins followed the predicted expression by gene array, though the delta differences were not always maintained, probably due to several mechanisms of protein synthesis and protein degradation.

Considering the importance of Wisp-2 as a regulatory element during adipocyte differentiation processes and the quantitative differences between control samples and TPTD-treated samples, the attention was focused on Wisp-2 protein to analyze in detail its localization and signaling.

To confirm the content of Wisp-2 upon TPTD treatment on osteocytes MLO-Y4 cells, we monitored the expression of Wisp-2 mRNA with specific primers. By means of quantitative qPCR we confirmed that Teriparatide was able to speed the level of Wisp-2 mRNA at 6 h; then it decreased consistently upon 9 h and 12. (Fig. 4).

By means of immunofluorescence, we monitored Wisp-2 localization and we recorded an increase of fluorescence positive cells related to Wisp-2 inside the cytosol upon 6 h of TPTD treatment (Fig. 5A and B). Therefore, we asked about the possible signaling mechanisms downstream TPTD, able to increase the amount of Wisp-2 in MLO-Y4 cells.

It is well known that TPTD is an active fraction of PTH hormone that, following the link with its receptor, induces β -catenin stabilization. β -catenin is an intermediate of WNT-pathway and upon stabilization in the cytoplasm, it translocates to the nucleus, interacts with TCF/LEF promoter and induces transcription of several genes involved in cell proliferation such as cyclin D1, c-myc, Axin and Wisp-1. Therefore, we asked whether also in our model TPTD was able to induce β -catenin nuclear translocation. By immunofluorescence analysis, we confirmed a clear staining of β -catenin in the nucleus and by western blot we monitored the increase of active non-phosphorylated β -catenin in nuclear extracts of cells treated with TPTD compared to untreated cells (Fig. 6A and B).

Since it is known that Wisp-2 is a glycosylated secreted protein, we tested the presence of Wisp-2 in MLO-Y4 medium. Upon TPTD treatment, we collected medium from MLO-Y4 cells treated/untreated with TPTD and we analyzed the presence of Wisp-2 in the medium. By means of western blot, we detected Wisp-2 protein, either in whole cell lysates either in media obtained by MLO-Y4 treated or not with the drug for 6 h. Next, we quantify Wisp-2 by Elisa Assay, confirming that Wisp-2 is secreted at higher level in media obtained by cells treated with TPTD

(Fig. 7A and B).

3.3. Conditioning of IDG-SW3 osteoblasts differentiation

To analyze if direct effect mediated by osteocyte-secreted-Wisp-2 occurs during the osteoblast to late osteocyte differentiation, we monitored by functional assays the differentiation of IDG-SW3 cells upon conditioning of their differentiation medium, firstly with medium obtained by MLO-Y4 osteocyte cells and secondly with Wisp-2 recombinant protein. As a first step, we analyzed the effect of MLO-Y4 cells medium (treated with TPTD for 0, 6, 9 and 12 h) during IDG-SW3 differentiation. Therefore, we maintained IDG-SW3 cells in osteogenic differentiation medium conditioned with medium from MLO-Y4 cells and we stopped the differentiation at 7 days (late osteoblast phenotype) at 14 days (early osteocyte phenotype) and at 21 days (late osteocyte phenotype). The results shown in panel (Fig. 8A–F) demonstrated that only at 7 days of IDG-SW3 differentiation there was a statistical significant difference between cells maintained in normal differentiation medium T0 compared to IDG-SW3 maintained in conditioned medium T6 and T9, suggesting a positive role of MLO-Y4 osteocyte medium treated with Teriparatide TPTD during osteogenic differentiation.

Since we hypothesized that the positive role induced by osteocyte MLO-Y4 conditioned medium treated with TPTD was attributed to Wisp-2 secreted protein, we conditioned the IDG-SW3 osteogenic differentiation (only in the first step at 7 days) with Wisp-2 recombinant protein. Data obtained by Alizarin red and ALP functional assays were very similar and demonstrated a strong and concentration-dependent Wisp-2 effect in increasing the mineralization process during osteoblast differentiation (Fig. 9A and B).

In order to verify whether this effect was specific for Wisp-2, we repeated the experiments using Wisp-2 recombinant protein complexed with a neutralization antibody. As expected, the increase of mineralization induced by Wisp-2 was completely abrogated upon the addition of the specific antibody (Fig. 9C).

To deeply analyze Wisp-2 ability to speed the osteogenesis process, we analyzed by real time PCR and Western blot the expression levels of some typical markers such as Sclerostin SOST, RUNX2 and DMP1, demonstrating an increment of these factors in cells conditioned by Wisp-2 (Fig. 10). Moreover, since we noted that the main effects induced by osteocyte medium on IDG-SW3 differentiation were visible at the early stage of osteogenic maturation (7 days of IDG-SW3 differentiation resembling the osteoblast phenotype) our further experiments were

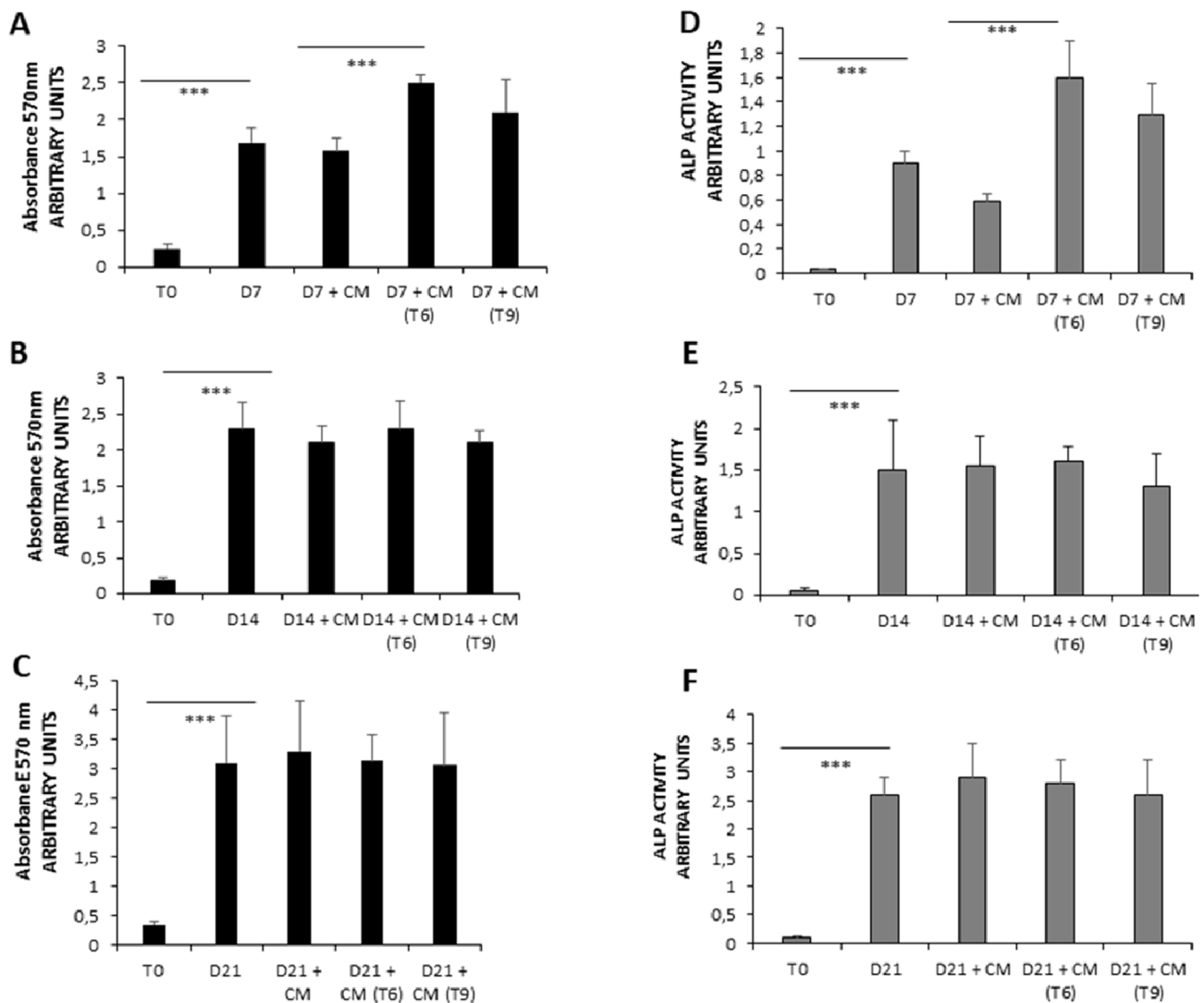


Fig. 8. IDG-SW3 were cultured in proliferating medium (T0) and in differentiating medium for 7 (A-D), 14 (B-E) or 21 (C-F) days. Where indicated, a quarter of the differentiating medium was added to MLO-Y4 medium (CM) treated with Teriparatide for 6h (T6) and 9h (T9). The respective controls were indicated as T0 representing IDG-SW3 cells maintained in proliferating medium. Quantification of Alizarin Red (A-B-C) staining and Alkaline Phosphatase activity were measured at 405 nm; (D, E, F). $***p < 0.005$, were calculated by the Student t-test.

performed on mesenchymal stem cells (MSCs) induced to osteogenic differentiation (Grisendi et al., 2011) Therefore, we cultured MSCs in a specific osteogenic medium added with recombinant Wisp-2 protein. Firstly, we checked whether MSCs were able to differentiate towards the osteogenic lineage (Fig. 11A and B) and secondly we added recombinant Wisp-2 to the differentiation medium.

ALP and Alizarin assays demonstrated that Wisp-2 increases the mineralization amount of interesting behavior in mesenchymal cells induced to osteogenic differentiation for 7 and 14 days, confirming its role in pushing the osteoblast differentiation process (Fig. 12A and B).

3.4. Wisp-2 expression and osteoblastic laminae extension in metaphyseal trabecular bone

In order to translate *in vivo* our *in vitro* data, we evaluated Wisp-2 expression by immunohistochemistry, in metaphyseal trabecular bone of the distal femurs of rats. We conducted this analysis on three animal groups, without/with TPTD treatment during normal diet restoration after 1 month calcium-free diet (see M&M). The distal femurs obtained by all the animals were analyzed for Wisp-2 expression in osteocytes inside the metaphyseal trabecular bone. We compared the same areas

among the group and we counted only the positive osteocytes (brown stained). The bar charts in Fig. 13 (A-B-C-D) show that the expression of positive cells for Wisp-2 is greater in group 3 (animals treated with TPTD) with respect to group 2 (animal untreated with TPTD), confirming the ability of the drug to induce an upregulation of the molecule in the osteocyte population. This result was in line with the finding observed by Hematoxylin and Eosin staining of the sequential sections, where we appreciated an increase of the extension of the surface of prismatic osteoblast laminae in group 3 comparing to group 2; the presence, revealed by the staining, of monostratified laminae of osteoblast polarized in the same direction (localized at the inner surface of the bone cavities) is a feature suggestive of active sites of bone deposition under TPTD administration. In fact, we detected significant higher osteoblast surface (16%) in group 3 with respect to group 2 (12%).

4. Discussion

The effect of TPTD on the osteogenesis as well as the involvement of osteocytes and their role in bone formation has been widely discussed, particularly in the last decade. It has already been demonstrated that

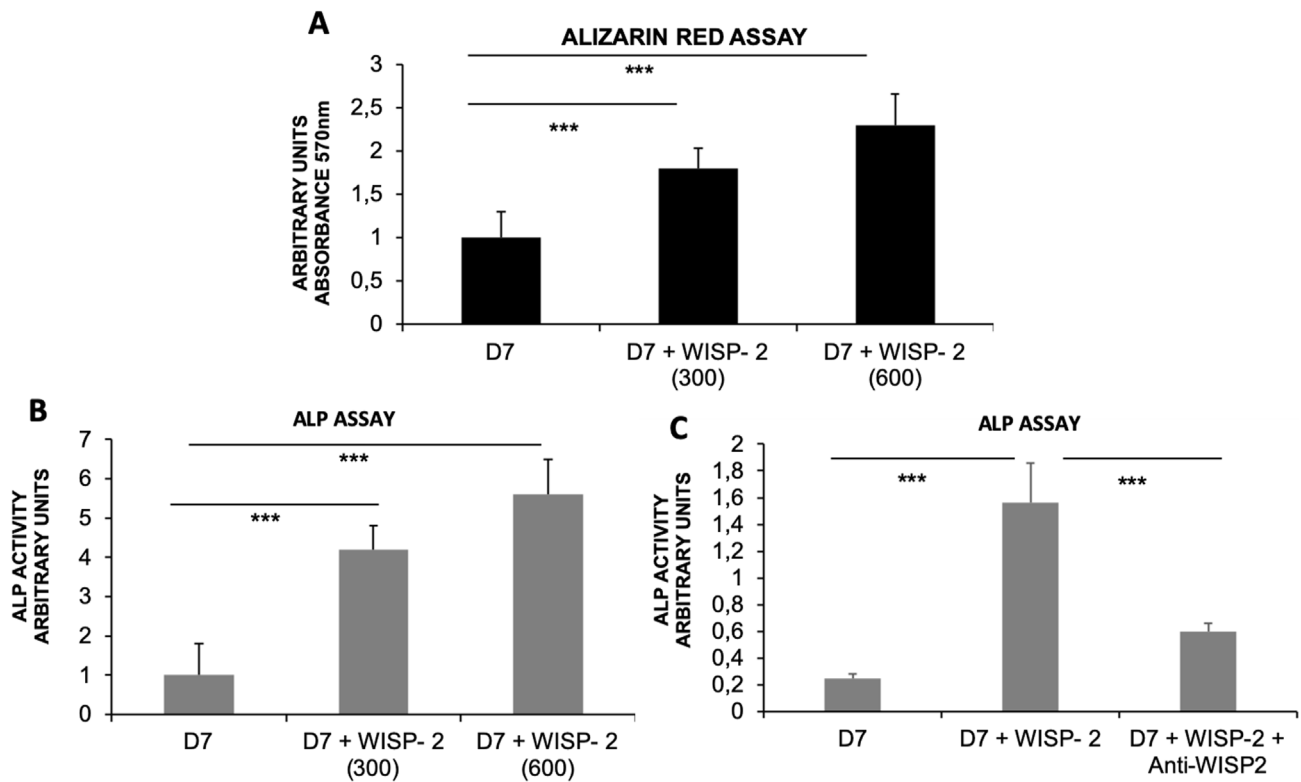


Fig. 9. Alizarin (A) and ALP (B) assays performed on IDG-SW3 cultured in differentiating medium for 7 days (D7) in presence of recombinant Wisp-2 protein at 300 ng/ml and 600 ng/ml. C: ALP assay performed on IDG-SW3 cells differentiated for 7 days in presence of recombinant Wisp2 at 300 ng/ml and in presence of a medium containing the complex formed by recombinant protein plus the respective neutralization antibody. Experiments were performed in triplicate. $***p < 0,005$ obtained by Student T-test.

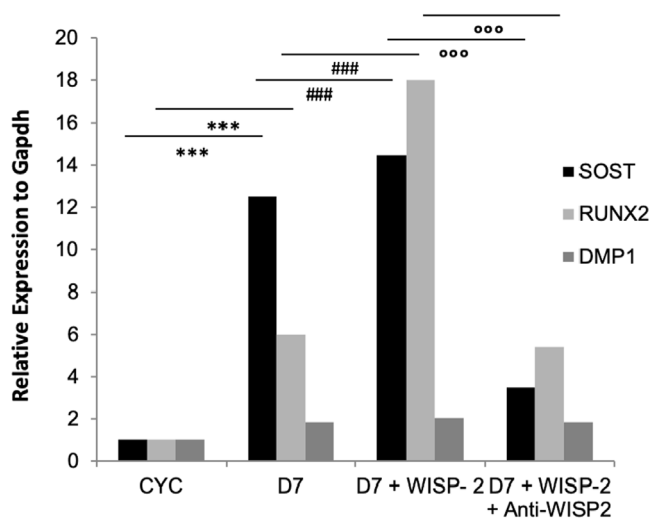


Fig. 10. IDG-SW3 were cultured in proliferating medium (CYC) and in differentiating medium for 7 days (D7). Where indicated recombinant WISP-2 (300 ng/ml) and the respective neutralization antibody were added to the medium. mRNA was extracted from the same samples described above and SOST, RUNX2 and DMP1 were analyzed by Real Time PCR. Fold change variation was calculated. The data are representative of three independent experiments. T student test was performed. CYC vs D7 $***p < 0,005$; D7 vs D7 + WISP2 $###p < 0,005$; D7 + WISP-2 vs D7 + anti WISP-2 $^{\circ}p < 0,005$.

intermittent administration of PTH (1-34) leads to bone deposition and bone growth, meanwhile continuous administration of PTH (1-34) exerts a catabolic effect characterized by an increase of osteoclast activation and bone resorption. Our study attempt to unveil a new molecule acting as an anabolic factor involved in speeding the osteogenic

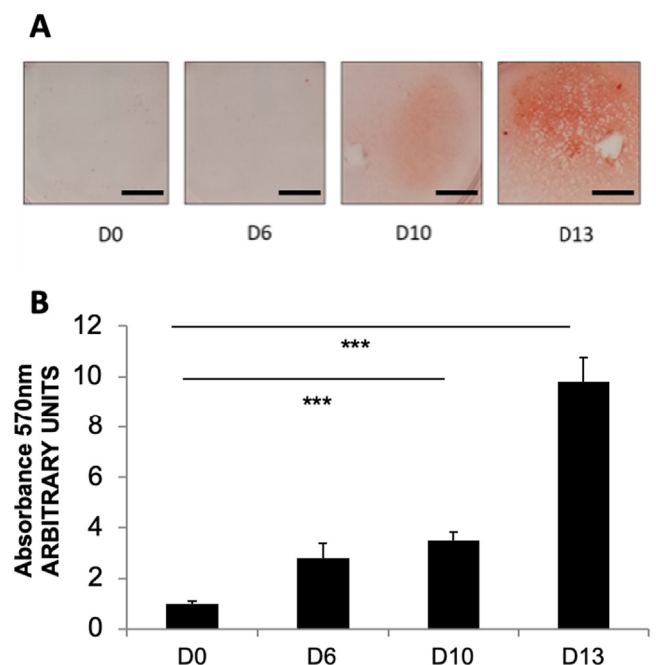


Fig. 11. Osteogenic differentiation of MSCs. A-B Cultured cells were stained with Alizarin Red S after 6, 10 and 13 days of differentiation to detect osteogenic induction. Scale bar = 50 μ m. For quantification, stains were solubilized and the absorbance was measured spectrophotometrically at 570 nm for 0.5 s (B). Bar charts shows fold change variations of absorbance values. All analyses were performed in triplicate. $***p < 0,005$ obtained by Student T-test.

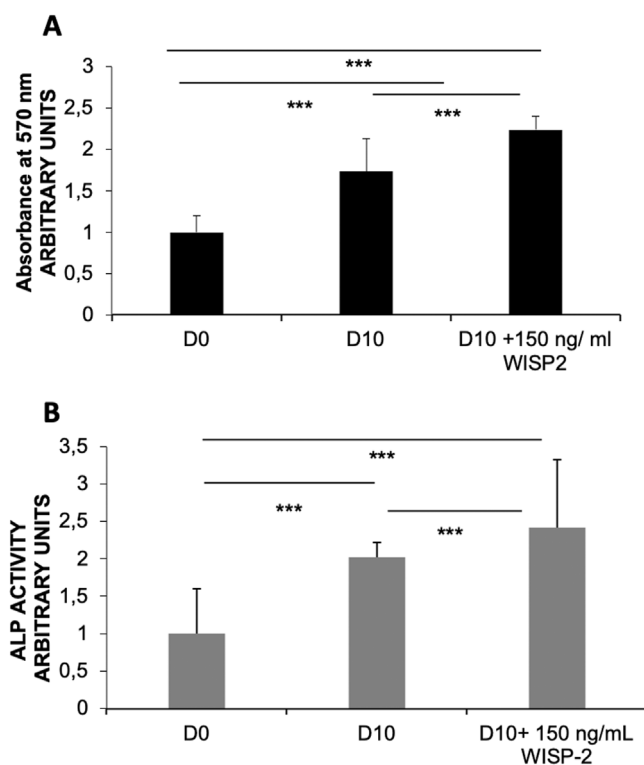


Fig. 12. A: MSCs were cultured in proliferating medium (D0) and in differentiating medium for 10 days (D10) implemented with recombinant Wisp 2 at a concentration of 150 ng/ml. At the indicated endpoints, cells were solubilized and the Alizarin Red stain was quantified at 570 nm. B: Analysis of ALP activity of the samples described above. The bar charts show differences expressed as Fold change variation. Experiments were performed in triplicate. *** $p < 0,005$ obtained by Student T-test.

process, observing fast and retard effects after 6, 9, and 12 h of TPTD treatment, by analyzing the expression of two typical bone turnover markers, osteoprotegerin and RUNX2, in MLO-Y4. As expected, osteoprotegerin and RUNX2 mRNA levels, increased upon 6 h of treatment, dropping upon 9 and 12 h at levels similar to the untreated condition.

Through the gene microarray technology, we showed, in a model of osteocyte like cells MLO-Y4, a significant alteration or changes in gene expression, induced by TPTD treatment. To avoid any possible bias, only those genes that showed a fold change higher than four were selected; this selective restriction allowed to obtain just the panel of 40 genes that showed an “inversion of expression”. The comparison between control and treatment samples, although showing a different expression of selected genes, does not reach the statistical significance.

Our working hypothesis was that among those genes could be included some genes related with the osteocyte cell signaling stimulated by TPTD. This particular “inversion of expression” may suggest that those genes could be some of the factors that may regulate the events occurring during TPTD treatment times mimicking anabolic to catabolic switch. A closer look at those 40 genes revealed that 13 of them were already well-known to exert biological/molecular function in bone. Among them, it was chosen to analyze by Western Blot the expression of proteins such as CTGF, PAI-1, WISP-2, CTSK and PTN. Among these proteins, the expression of Wisp-2 showed an interesting behavior. Wisp-2 is a member of the CCN family and a factor of the Wnt pathway that positively regulates the osteoblast differentiation; a marked increment of its expression level after 6 h of treatment was observed compared to control; also, after 9 and 12 h of treatment with TPTD, Wisp-2 expression level was comparable to the control level. Using our original model, we showed that the fast effect of TPTD leads to an increase in the production of the Wisp-2 protein, which can be one

of the molecular regulators able to stimulate osteoblast differentiation. The levels of Wisp-2 protein decreased already after 9 h of treatment and reached levels comparable to control after 12 h. Wisp-2 is a canonical Wnt ligand that regulates cell proliferation, adhesion and differentiation, in particular secreted Wisp-2 promotes mesenchymal precursor cell proliferation and maintains the cells in undifferentiated state. In bone-forming osteoblasts, Wisp-2 promotes adhesion and inhibits osteocalcin production (Grünberg et al., 2014; Hammarstedt et al., 2013; Ono et al., 2011). Thus, analyzing in detail the role of this interesting protein, it emerged that not only the expression of mRNA as well as protein of Wisp-2 were increased upon 6 h of treatment, but also that the secreted form, detectable in the cultured osteocyte conditioned medium, was increased upon the same time of treatment. These data strongly suggest that secreted Wisp-2, fast induced by TPTD treatment, could be an important factor involved in the activation of different signaling pathways. Based on these findings, osteocyte-derived culture medium was used to condition the osteoblast IDG-SW3 during their differentiation. The mineralizing ability of IDG-SW3 induced to differentiate, under the conditioning effects of MLO-Y4 culture medium, was analyzed by Alizarin Red and ALP assays. Functional assay of mineralization brings clues on how TPTD influences osteocyte in expressing factors that indirectly stimulate bone cell differentiation and mineralization. After 7 days of culture, when the phenotype of IDG-SW3 resembles the early steps of osteogenic differentiation, an increase of mineralization was observed for all the groups and it is interesting to highlight how the longer time point (12 h), even though it was higher respect to the control, has an opposite trend compared to the other two time points selected (6 and 9 h). After 14 and 21 days of differentiation (points that mimic the early and late osteocyte phenotype, respectively), only the 6 h treatment was found to induce modifications statistically significant. This result is clearly in agreement with our hypothesis concerning both *i*) indirect effects mediated by osteocytes on osteoblast differentiation process; *ii*) time-dependent effect of the drug on osteocytes. All together, these data showed an interesting behavior expressed by the *in vitro* osteocyte-like cell line model MLO-Y4, treated at different time points, during IDG-SW3 osteoblast differentiation: in particular, it is of note that our data point out the role of secreted factors, such as Wisp-2, in controlling the fate of osteoblast maturation. As proof of this finding, it was recently identified by Joeng and coworkers an anabolic function of osteocytes as a source of Wnt in bone development and homeostasis, complementing their known function as targets of Wnt signaling in regulating osteoclastogenesis and osteoblastogenesis (Joeng et al., 2017).

To substantiate the interesting data obtained *in vitro*, regarding WISP-2 positive role on osteogenesis, we performed immunohistochemical and histomorphometrical analyses in metaphyseal trabecular bone of the distal femurs of PTH treated/untreated rats, concerning either Wisp-2 expression or the presence/extension of osteoblast laminae. Both these evaluations strongly indicate that one of the possible mechanisms controlling TPTD anabolic role, is the WISP-2 up-regulation. This datum is in line with a recent work by Ferretti and coworkers (Ferretti et al., 2019) demonstrating that PTH(1-34) was actively involved in enhancing bone mass recovery, particularly in trabecular bone depleted after calcium deprivation. In the present study, as expected, a consistent decrease (about 25.5%) of osteoblast laminae surface in rats maintained in calcium-free diet occurs; such decrement is partially recovered upon the TPTD administration, in fact we found that the number of osteoblast laminae surface was increased (about 15,15%) following the active bone deposition triggering induced by the drug. All these data highlighted the importance of Wisp-2 produced by osteocyte population in pushing osteogenesis process. Our results match also with the observations by Cavani and coworkers (Cavani et al., 2017) on PTH(1-34) effects during repairing experimentally drilled holes in rat femur, where the main effect of PTH(1-34) was demonstrated to be the induction of a faster healing of the bone lesions with respect to the injured rats that not underwent PTH

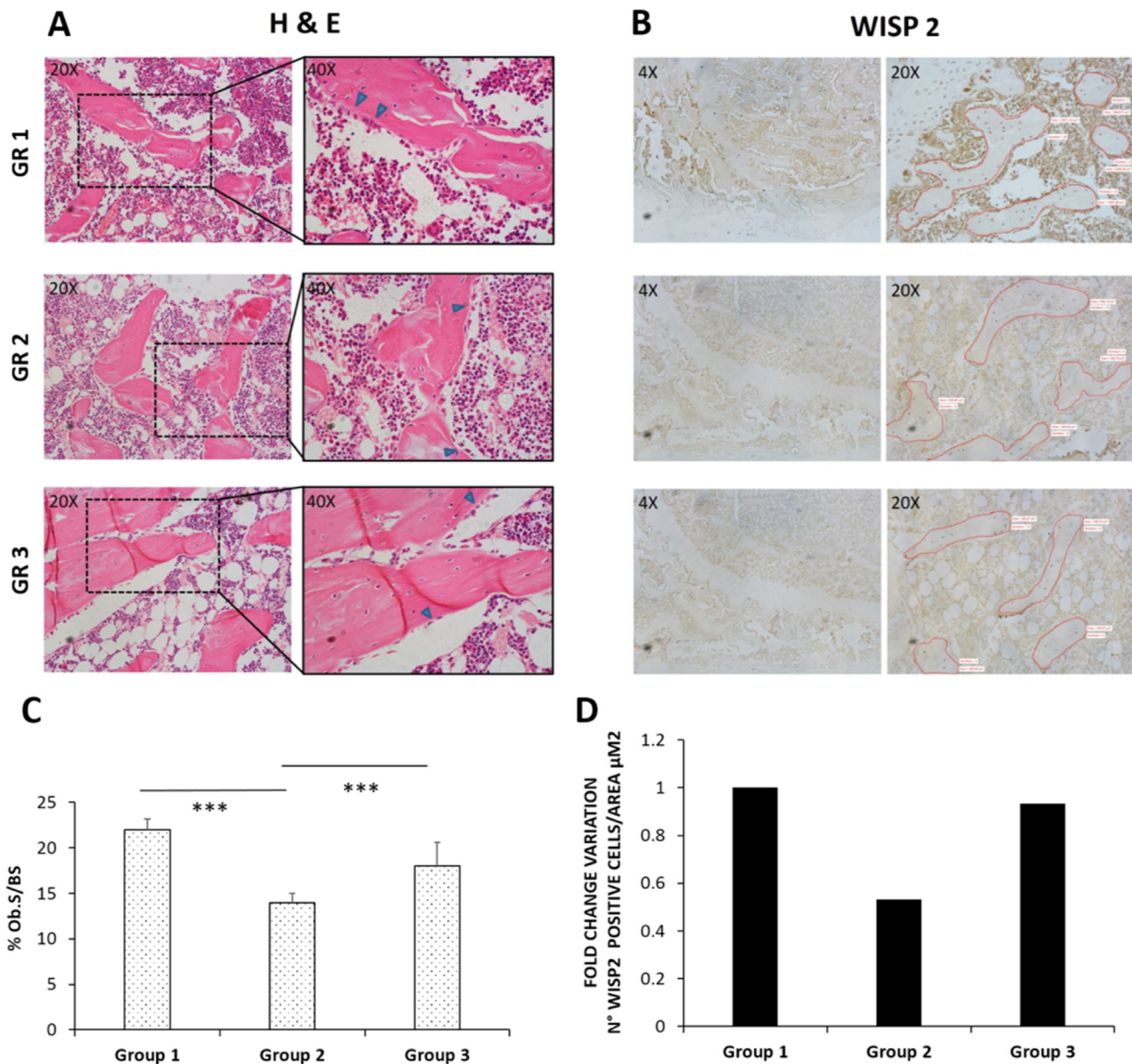


Fig. 13. A: H & E staining of 4 μ m sections of femurs distal metaphyseal trabecular bones. The images are representative of 10 counted fields for three animals per group. GR1: control animals (2 month); GR2: animals fed with Calcium deprived diet (1 month) and restored with normal diet (1 month) and treated with Teriparatide. Head-arrows indicate the presence of prismatic osteoblast laminae. B: Immunohistochemistry of WISP2 in 4 μ m sections of femurs distal metaphyseal trabecular bones. The images are representative of 10 counted fields for three animals per group. Brown cells are positively DAB stained. GR1-GR2 and GR3 are described in H&E caption. The red areas represent the trabecular bone where only the positive brown osteocytes were counted. C: Quantification of H&E stained prismatic osteoblast laminae. The evaluation was performed counting the length of osteoblast (inside the laminae) respect to the extent of the bone surface. The values in the bar chart are expressed in percentage (Ob.S/BS). The errors bars represent the Standard Deviation. The count was performed on sections obtained by three independent animals. D: Quantification of the total number of positive osteocytes inside the trabecular bone areas. N = 10 fields per slide for three animals have been evaluated. No statistical differences are showed. $***p < 0,005$ obtained by Student T-test.

administration.

In conclusion, the main original findings emerging from the present work are: *i*) TPTD is able to induce in osteocyte model the modulation of genes in fast or retard timing, so that while several genes are fast affected, considerably less changes are detectable as retard effect of the drug *ii*) soluble factors, such as Wisp-2, induced by the activation of Wnt pathway in osteocytes, are crucially involved in the fate of osteoblast differentiation process.

Author contributions

Alberto Smargiassi and Jessika Bertacchini conceived and designed the experiments; Alberto Smargiassi, Marta Checchi, Francesco Potì, Giulia Grisendi, Elena Tenedini, Giuliana Montosi, Maria Sara Magarò, Marzia Ferretti and Francesco Cavani performed the experiments; Alberto Smargiassi, Jessika Bertacchini, Delphine B. Maurel and Carla Palumbo wrote the paper and Carla Palumbo recruited the funds.

CRedit authorship contribution statement

Alberto Smargiassi: Conceptualization, Methodology, Validation, Investigation, Formal analysis, Writing - original draft. **Jessika Bertacchini:** Conceptualization, Data curation, Writing - original draft, Writing - review & editing. **Marta Checchi:** Methodology, Validation, Investigation, Formal analysis. **Francesco Potì:** Methodology, Validation, Investigation, Formal analysis. **Elena Tenedini:** Methodology, Validation, Investigation, Formal analysis. **Giuliana Montosi:** Methodology, Validation, Investigation, Formal analysis. **Maria Sara Magarò:** Methodology, Validation, Investigation, Formal analysis. **Francesco Cavani:** Methodology, Validation, Investigation, Formal analysis. **Marzia Ferretti:** Methodology, Validation, Investigation, Formal analysis. **Grisendi Giulia:** Methodology, Validation, Investigation, Formal analysis. **Delphine B. Maurel:** Data curation, Writing - original draft, Writing - review & editing. **Carla Palumbo:** Writing - original draft, Funding acquisition.

Declaration of competing interest

The authors declare no conflict of interest.

Acknowledgments

The authors wish to thank Professors Antonello Pietrangelo (Center for Hemochromatosis, UNIMORE) and Enrico Tagliafico (Center for Genome Research, UNIMORE) for making their laboratories available for the gene array and PCR-analysis.

This study was supported by funds from the University of Modena and Reggio Emilia, Departmental grant FAR 2015-FAR 2017. Grant from Eli-Lilly (U.S.A). The study was also supported by funds "Department of Excellence 2018-2021" (Department of Biomedical, Metabolic and Neural Sciences).

References

- Angers, S., Moon, R.T., 2009. Proximal ev1. Angers, S. & Moon, R. T. Proximal events in Wnt signal transduction. *Nat. Rev. Mol. Cell Biol.* 10, 468–477. <https://doi.org/10.1038/nrm2717>. (2009).ents in Wnt signal transduction. *Nat. Rev. Mol. Cell Biol.*
- Bellido, T., Saini, V., Pajevic, P.D., 2013. Effects of PTH on osteocyte function. *Bone* 54, 250–257. <https://doi.org/10.1016/j.bone.2012.09.016>.
- Bertacchini, J., Benincasa, M., Checchi, M., Cavani, F., Smargiassi, A., Ferretti, M., Palumbo, C., 2017. Expression and functional proteomic analyses of osteocytes from *Xenopus laevis* tested under mechanical stress conditions: preliminary observations on an appropriate new animal model. *J. Anat.* 231, 823–834. <https://doi.org/10.1111/joa.12685>.
- Bertacchini, J., Magarò, M.S., Potì, F., Palumbo, C., 2018. Osteocytes specific GSK3 inhibition affects in vitro osteogenic differentiation. *Biomedicines* 6, 61. <https://doi.org/10.3390/biomedicines6020061>.
- Bonewald, L.F., 2011. The amazing osteocyte. *J. Bone Miner. Res.* 26, 229–238. <https://doi.org/10.1002/jbmr.320>.
- Cavani, F., Ferretti, M., Smargiassi, A., Palumbo, C., 2017. PTH(1-34) effects on repairing experimentally drilled holes in rat femur: novel aspects – qualitative vs. quantitative improvement of osteogenesis. *J. Anat.* 230, 75–84. <https://doi.org/10.1111/joa.12533>.
- Dodds, R. a, Ali, N., Pead, M.J., Lanyon, L.E., 1993. Early loading-related changes in the activity of glucose 6-phosphate dehydrogenase and alkaline phosphatase in osteocytes and periosteal osteoblasts in rat fibulae in vivo. *J. Bone Miner. Res.* 8, 261–267. <https://doi.org/10.1002/jbmr.5650080303>.
- Ferretti, M., Cavani, F., Roli, L., Checchi, M., Magarò, M.S., Bertacchini, J., Palumbo, C., 2019. Interaction among calcium diet content, PTH (1-34) treatment and balance of bone homeostasis in rat model: the trabecular bone as keystone. *Int. J. Mol. Sci.* 20. <https://doi.org/10.3390/ijms20030753>.
- Giannotti, S., Bottai, V., Dell'Osso, G., Pini, E., De Paola, G., Bugelli, G., Guido, G., 2013. Current medical treatment strategies concerning fracture healing. *Clin. Cases Miner. Bone Metab.* 10, 116–120. <https://doi.org/10.1138/ccmbm/2013.10.2.116>.
- Grisendi, G., Bussolari, R., Cafarelli, L., Petak, I., Rasini, V., Veronesi, E., De Santis, G., Spano, C., Tagliazzucchi, M., Barti-Juhász, H., Scarabelli, L., Bambi, F., Frassoldati, A., Rossi, G., Casali, C., Morandi, U., Horwitz, E.M., Paolucci, P., Conte, P., Domini, M., 2011. Therapeutic potential of human mesenchymal stem cells producing Il-12 in a mouse xenograft model of renal cell carcinoma. *J. Urol.* 185, 751. <https://doi.org/10.1016/j.juro.2010.10.008>.
- Grünberg, J.R., Hammarstedt, A., Hedjazifar, S., Smith, U., 2014. The novel secreted adipokine wnt1-inducible signaling pathway protein 2 (WISP2) is a mesenchymal cell activator of canonical WNT. *J. Biol. Chem.* 289, 6899–6907. <https://doi.org/10.1074/jbc.M113.51964>.
- Guimarães, G.N., Stipp, R.N., Rodrigues, T.L., De Souza, A.P., Line, S.R.P., Marques, M.R., 2013. Evaluation of the effects of transient or continuous PTH administration to odontoblast-like cells. *Arch. Oral Biol.* 58 <https://doi.org/10.1016/j.archoralbio.2012.11.011>. 683–645.
- Hadjidakis, D., Androulakis, I.I., 2006. Bone remodeling. *Ann. N. Y. Acad. Sci.* 1092, 385–396. <https://doi.org/10.1196/annals.1365.035>.
- Hammarstedt, A., Hedjazifar, S., Jenndahl, L., Gogg, S., Grünberg, J., Gustafson, B., Klimcakova, E., Stich, V., Langin, D., Laakso, M., Smith, U., 2013. WISP2 regulates preadipocyte commitment and PPAR γ activation by BMP4. *Proc. Natl. Acad. Sci. U.S.A.* 110, 2563–2568. <https://doi.org/10.1073/pnas.1211255110>.
- Hao, Z., Ma, Y., Wu, J., Li, X., Chen, H., Shen, J., Wang, H., 2017. Osteocytes regulate osteoblast differentiation and osteoclast activity through Interleukin-6 under mechanical loading. *RSC Adv.* 7, 50200–50209. <https://doi.org/10.1039/c7ra09308j>.
- Iida-Klein, A., Lu, S.S., Kapadia, R., Burkhardt, M., Moreno, A., Dempster, D.W., Lindsay, R., 2005. Short-term continuous infusion of human parathyroid hormone 1-34 fragment is catabolic with decreased trabecular connectivity density accompanied by hypercalcemia in C57BL/6 mice. *J. Endocrinol.* 186, 549–557. <https://doi.org/10.1677/joe.1.06270>.
- Jilka, R.L., 2007. Molecular and cellular mechanisms of the anabolic effect of intermittent PTH. *Bone* 40, 1434–1436. <https://doi.org/10.1016/j.bone.2007.03.017>.
- Joeng, K.S., Lee, Y.C., Lim, J., Chen, Y., Jiang, M.M., Munivez, E., Ambrose, C., Lee, B.H., 2017. Osteocyte-specific WNT1 regulates osteoblast function during bone homeostasis. *J. Clin. Invest.* 127, 2678–2688. <https://doi.org/10.1172/JCI92617>.
- Kim, S.W., Pajevic, P.D., Selig, M., Barry, K.J., Yang, J.Y., Shin, C.S., Baek, W.Y., Kim, J.E., Kronenberg, H.M., 2012. Intermittent parathyroid hormone administration converts quiescent lining cells to active osteoblasts. *J. Bone Miner. Res.* 27, 2075–2084. <https://doi.org/10.1002/jbmr.1665>.
- Livak, K.J., Schmittgen, T.D., 2001. Analysis of relative gene expression data using real-time quantitative PCR and the 2- $\Delta\Delta$ CT method. *Methods* 25, 402–408. <https://doi.org/10.1006/meth.2001.1262>.
- MacDonald, B.T., Tamai, K., He, X., 2009. Wnt/beta-catenin signaling: components, mechanisms, and diseases. *Dev. Cell* 17, 9–26. <https://doi.org/10.1016/j.devcel.2009.06.016>.
- Mao, J., Wang, J., Liu, B., Pan, W., Farr, G.H., Flynn, C., Yuan, H., Takada, S., Kimelman, D., Li, L., Wu, D., 2001. Low-density lipoprotein receptor-related protein-5 binds to Axin and regulates the canonical Wnt signaling pathway. *Mol. Cell* 7, 801–809. [https://doi.org/10.1016/S1097-2765\(01\)00224-6](https://doi.org/10.1016/S1097-2765(01)00224-6).
- Marotti, G., Palumbo, C., 2007. The mechanism of transduction of mechanical strains into biological signals at the bone cellular level. *Eur. J. Histochem.* 51 (Suppl. 1), 15–19.
- Maycas, M., Ardura, J.A., De Castro, L.F., Bravo, B., Gortázar, A.R., Esbrit, P., 2015. Role of the parathyroid hormone type 1 receptor (PTH1R) as a mechanosensor in osteocyte survival. *J. Bone Miner. Res.* 30, 1231–1244. <https://doi.org/10.1002/jbmr.2439>.
- Nakashima, T., Hayash, M., Takayanagi, H., 2012. [Regulation of bone resorption by osteocytes]. *Clin. Calcium* 22, 685–696.
- Nakashima, T., Hayashi, M., Fukunaga, T., Kurata, K., Oh-Hora, M., Feng, J.Q., Bonewald, L.F., Kodama, T., Wutz, A., Wagner, E.F., Penninger, J.M., Takayanagi, H., 2011. Evidence for osteocyte regulation of bone homeostasis through RANKL expression. *Nat. Med.* 17, 1231–1234. <https://doi.org/10.1038/nm.2452>.
- Neer, R.M., Arnard, C.D., Zanchetta, J.R., Prince, R., Gaich, G.A., Reginster, J.Y., Hodsman, A.B., Eriksen, E.F., Ish-Shalom, S., Genant, H.K., Wang, O., Mittlek, B.H., Mellström, D., Oefjord, E.S., Marcinowska-Suchowierska, E., Salmi, J., Mulder, H., Halse, J., Sawicki, A.Z., 2001. Effect of parathyroid hormone (1-34) on fractures and bone mineral density in postmenopausal women with osteoporosis. *N. Engl. J. Med.* 344, 1434–1441. <https://doi.org/10.1056/NEJM200105103441904>.
- Ono, M., Inkson, C.A., Kilts, T.M., Young, M.F., 2011. WISP-1/CCN4 regulates osteogenesis by enhancing BMP-2 activity. *J. Bone Miner. Res.* 26, 193–208. <https://doi.org/10.1002/jbmr.205>.
- Osagie-Clouard, L., Sanghani, A., Coathup, M., Briggs, T., Bostrom, M., Blunn, G., 2017. Parathyroid hormone 1-34 and skeletal anabolic action. *Bone Joint Res.* 6, 14–21. <https://doi.org/10.1302/2046-3758.6.1.bjr-2016-0085.r1>.
- Pietrzyk, B., Smertka, M., Chudek, J., 2017. Sclerostin: intracellular mechanisms of action and its role in the pathogenesis of skeletal and vascular disorders. *Adv. Clin. Exp. Med.* 26, 1283–1291. <https://doi.org/10.17219/acem/68739>.
- Poole, K.E.S., Reeve, J., 2005. Parathyroid hormone - a bone anabolic and catabolic agent. *Curr. Opin. Pharmacol.* 5, 612–617. <https://doi.org/10.1016/j.coph.2005.07.004>.
- Raggatt, L.J., Partridge, N.C., 2010. Cellular and molecular mechanisms of bone remodeling. *J. Biol. Chem.* 285, 25103–25108. <https://doi.org/10.1074/jbc.R109.041087>.
- Riek, A.E., Towler, D.A., 2011. The pharmacological management of osteoporosis. *Mo. Med.* 108, 118–123.
- Robinson, J.A., Chatterjee-Kishore, M., Yaworsky, P.J., Cullen, D.M., Zhao, W., Li, C., Kharode, Y., Sauter, L., Babij, P., Brown, E.L., Hill, A.A., Akhter, M.P., Johnson, M.L., Recker, R.R., Komm, B.S., Bex, F.J., 2006. Wnt/ β -catenin signaling is a normal physiological response to mechanical loading in bone. *J. Biol. Chem.* 281, 31720–31728. <https://doi.org/10.1074/jbc.M602308200>.
- Sims, N.A., Walsh, N.C., 2012. Intercellular cross-talk among bone cells: new factors and pathways. *Curr. Osteoporos. Rep.* 10, 109–117. <https://doi.org/10.1007/s11914-012-0096-1>.
- Skerry, T.M., Bitensky, L., Chayen, J., Lanyon, L.E., 1989a. Early strain-related changes in enzyme activity in osteocytes following bone loading in vivo. *J. Bone Miner. Res.* 4, 783–788. <https://doi.org/10.1002/jbmr.5650040519>.
- Skerry, Timothy M., Lanyon, L.E., Bitensky, L., Chayen, J., 1989b. Early strain-related

- changes in enzyme activity in osteocytes following bone loading in vivo. *J. Bone Miner. Res.* 4, 783–786. <https://doi.org/10.1002/jbmr.5650040519>.
- Sugiura, T., Kashii, M., Matsuo, Y., Morimoto, T., Honda, H., Kaito, T., Iwasaki, M., Yoshikawa, H., 2015. Intermittent administration of teriparatide enhances graft bone healing and accelerates spinal fusion in rats with glucocorticoid-induced osteoporosis. *Spine J.* 15, 298–306. <https://doi.org/10.1016/j.spinee.2014.08.001>.
- Tatsumi, S., Ishii, K., Amizuka, N., Li, M., Kobayashi, T., Kohno, K., Ito, M., Takeshita, S., Ikeda, K., 2007. Targeted ablation of osteocytes induces osteoporosis with defective mechanotransduction. *Cell Metabol.* 5, 464–475. <https://doi.org/10.1016/j.cmet.2007.05.001>.
- Vezeridis, P.S., Semeins, C.M., Chen, Q., Klein-Nulend, J., 2006. Osteocytes subjected to pulsating fluid flow regulate osteoblast proliferation and differentiation. *Biochem. Biophys. Res. Commun.* 348, 1082–1088. <https://doi.org/10.1016/j.bbrc.2006.07.146>.
- Weinstein, R.S., O'Brien, C.A., Almeida, M., Zhao, H., Roberson, P.K., Jilka, R.L., Manolagas, S.C., 2011. Osteoprotegerin prevents glucocorticoid-induced osteocyte apoptosis in mice. *Endocrinology* 152, 3323–3331. <https://doi.org/10.1210/en.2011-0170>.
- Woo, S.M., Rosser, J., Dusevich, V., Kalajzic, I., Bonewald, L.F., 2011. Cell line IDG-SW3 replicates osteoblast-to-late-osteocyte differentiation in vitro and accelerates bone formation in vivo. *J. Bone Miner. Res.* 26, 2634–2646. <https://doi.org/10.1002/jbmr.465>.
- Xiong, J., Piemontese, M., Thostenson, J.D., Weinstein, R.S., Manolagas, S.C., O'Brien, C.A., 2014. Osteocyte-derived RANKL is a critical mediator of the increased bone resorption caused by dietary calcium deficiency. *Bone* 66, 146–154. <https://doi.org/10.1016/j.bone.2014.06.006>.